

# Preliminary Design and Performance Assessment of Electric VTOL Blended Wing Body Aircraft

Deepak Poudel

Researcher, Department of Aerospace Engineering  
Gandhi Institute of Technology and Management  
Hyderabad, India

Bijay Pal

Department of Electrical Engineering  
Government College of Engineering  
Keonjhar, India

**Abstract**—Aeronautics researchers have been seeking the solution for sustainable aviation for a long time and the research and development of electric Vertical Take Off and Landing (eVTOL) aircrafts to facilitate the Urban Air Mobility (UAM) and Regional Air Mobility (RAM) markets have gained a lot of interest recently with the improvement in battery technology. Similarly, parallel research has been going on the design of Blended Wing Body (BWB) aircraft for long haul markets. But the research on the integration of BWB concept with eVTOL capability for lower subsonic speed is lacking. Thus, this research is initiated to develop a conceptual design framework for eVTOL BWB aircraft configuration and to conduct the preliminary performance evaluation to determine its feasibility for UAM and RAM market. For this 6-seater aircraft with range capacity of 250 KM+ is designed. Market analysis and design studies is conducted to set the general requirements of the aircraft suited for the market. Similarly, the existing mathematical models for hovercrafts and fixed wing aircrafts are modified for performance assessment of the intended design. In this research, initial criteria and mathematical framework is developed and evaluated and preliminary assessment of aerodynamic performance of the aircraft is estimated using computational fluid dynamic tools.

**Keywords**—Blended Wing Body; eVTOL; Regional Air Mobility; electric propulsion; aerodynamic assessment

## I. INTRODUCTION

The scope of short haul aviation market primarily Urban Air Mobility (UAM) and Regional Air Mobility (RAM) has been investigated by aviation giants as well as by new aeronautics start-ups to introduce a more reliable, safer and, environmentally friendly solution in the field of aviation. The UAM market demands the operating range of 5-40 km at the cruising velocity of 19 m/s to 35 m/s whereas, RAM market requires the operating range of about 100-300 km and speed exceeding 200 m/s [1]. Similarly, BWB aircraft initially purposed by Robert H. Liebeck represented a potential breakthrough in subsonic transport efficiency with 15% reduction in takeoff weight and a 27% reduction in fuel burn per seat mile [2]. Other advantages of the BWB design encompass 15-20% increase in lift to drag ratio due to the reduction of the parasite drag [2]. Based on literature review, the possible advantage of BWB aircraft configuration include reduction in weight, increased fuel efficiency, reduction in noise and NO<sub>x</sub> emissions as well as larger payload volume. Unlike problems like cabin pressurization and structural integrity associated with BWB aircraft for commercial airliners, it can simply be omitted for eVTOL concept simply by cruising at lower altitude. Various configurations of

eVTOL aircrafts are under research and development. The most common configuration use horizontally mounted fans as the source of lift with is similar to conventional drones but it can limit the cruising speed and range of aircraft. Some groups of aircrafts use thrust vectoring i.e ducted fans or rotating wings and they offer longer range and faster cruise speed compared to fixed motor configurations. Reference [3] suggests that ducted fans increase the thrust and reduce noise for a motor with the same output. On the other hand, [4] examines that these ducted fans can add weight and drag to the design. Similarly, [5] examines the advantages of tilt-wing designs mentioning that they allow for reduced drag during the cruising phase of the flight in comparison with fixed rotor design. Reference [6] conducted an extensive review of research in urban on-demand air mobility and current technology. The research found that horizontally mounted props require far less power than the thrust vectoring design however the research also presented that the passenger carrying capacity of thrust vectoring aircraft was higher than of multicopters. But the fuselage and wing configuration trend for eVTOL aircraft is diverging and large number of unconventional configurations have been tested by industries and researchers. For on-demand UAM, electric propulsion is more optimal than that of gas-powered propulsion. Reference [7] suggest that electric motors have higher thrust to weight ratio in comparison to gas turbine engines due to reduction of heavier components. Similarly, the scaling up or scaling down of electric engines is much easier because of their simplicity providing designers with flexibility to solve power requirements as well as aerodynamic and structural challenges. These additional advantages including sustainability and lesser environmental impacts of eVTOL aircraft has transformed these aircrafts as the future for UAM and RAM markets.

## II. MARKET ANALYSIS AND MANUFACTURING POTENTIAL

Efficient aerodynamics of BWB aircraft compared to conventional tube and wing aircraft results in 10-20% reduction in direct operating cost [2] and thus it has the capacity to increase the revenue yielding payload. Even though there is no statistical data available for reduction in battery energy storage due to BWB design we can infer that the lower power requirement resulting lesser battery weight from the reduced fuel burn analysis. Current projection from the AIAA [8] shows that more than 660 million people will use eVTOL UAVs by 2035. This paper also projects the dropping of cost per passenger mile to \$ 0.20 in the same time

frame. Similarly, the study conducted by Uber outlining their vision for on-demand aviation service examines eVTOL aircraft as existing transport solutions for urban mobility.

BWB aircraft does not incorporate empennage reducing complex wing to fuselage and wing to empennage joints leading to fewer parts counts and it results in the reduction of difficulties during manufacturing. But it requires a thick center body airfoil section as per the cabin volume requirement which creates challenges for airfoil design and manufacturing while maintaining a low profile drag. The battery technology is expected to improve with energy density of around 400 Wh/Kg becoming available during the period of development of aircraft in 2023- 2027. Thus, the manufacturing and development of eVTOL BWB aircraft.

### III. DESIGN REQUIREMENTS

The general requirements of the aircraft investigated by design studies based on market analysis, certification requirements set by civil aviation regulatory bodies along with sustainability kept at the focal point are summarized below.

- Must be able to transport 7 people (1 pilot and 6 passengers), each person weighing 80 kg (+10 kg luggage for each passenger)
- Must be able to take-off and land vertically, as well as hover
- Minimum cruising altitude of 500 m
- Must have range of 200 km
- CS-23 level 3 certification
- Must satisfy the sustainable aviation goal with zero carbon footprint and reduction in noise

### IV. INITIAL SIZING

#### A. Statistical Study

The initial sizing of the aircraft is based on statistical data of similar aircraft configuration. The performance data of different eVTOL and Hybrid Electric Propulsion aircraft is obtained through the extensive online research and is presented below in Fig 1.

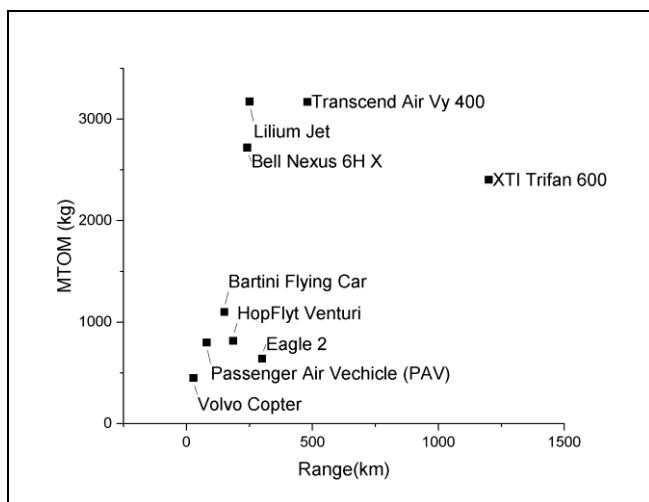


Fig. 1 Range-MTOW data of similar aircrafts

Lilium jet is chosen as the reference aircraft owing to its effectivity in UAM and RAM markets. The specifications of the reference aircraft are presented in Table 1.

Table 1. Reference aircraft performance data

Specification	Data
Payload	1 Pilot + 6 Passenger
Propulsion	36 Ducted fans and electric motors (DEVT)
MTOM	3175 kg
Wing Span	13.9 m
Range	250+ km
Cruising Speed	280 km/hr.
Endurance	60 mins
Cruising Altitude	3000 m

#### B. Weight Estimation

Initial mass approximation is done by adding 10% extra mass to reference aircraft mass per passenger. Payload weight is calculated being based on CS 23 regulations for 6- seater aircraft configuration. Similarly, battery weigh is approximated using the description given in [9]. The specific density of the battery is assumed to be 400 W-hr./kg and lift to drag ratio to be 20 which resulted in the mass ratio  $\frac{W_B}{MTOW}$  of 0.3. The empirical formulae [10] is used for mass estimation of other aircraft components and is presented in Fig. 2. The MTOW of the aircraft is calculated to be 3266 kg.

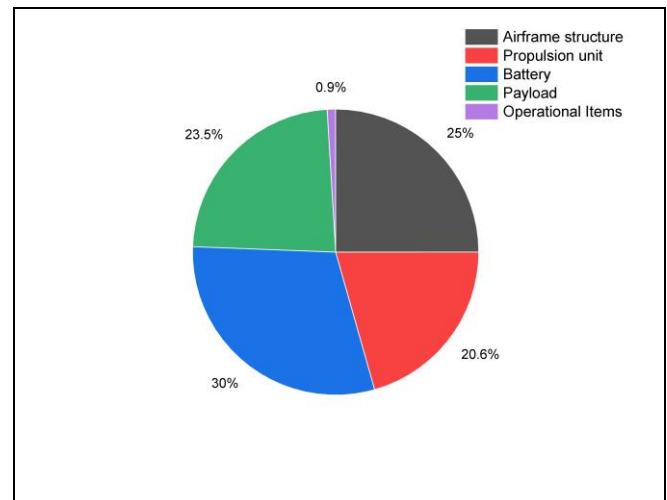


Fig. 2 Mass breakdown for eVTOL BWB aircraft

#### C. Preliminary estimation of flight performance

The calculation of thrust to weight ratio and wing loading is important at this stage which provide the basis for wing sizing as well as battery power requirement. The choice of various aerodynamic parameters to be introduced subsequently are constrained by both certification requirement and design objectives.

Number of crew and passenger: The aircraft is designed for 1 pilot and 6 passengers. Payload subject to change in case of emergency services.

Engines: The aircraft will use distributed electric propulsion to combine forward propulsion with its eVTOL capabilities.

Maximum Takeoff Weight: The MTOW of the aircraft is calculated to be 3266 kg or 32007 N.

Cruising Speed, Stalling Speed, Altitude and Turn Load: The cruising speed of the aircraft is 83.3 m/s and the cruising altitude is 3000m. The values are obtained from the tradeoff studies of existing aircraft data from the literature. The stalling speed of the aircraft is 33.5 m/s as per CS 23. Similarly, the turn load is related to roll i.e bank angle and as per CS 23.157, the maximum bank angle is

$$\phi = 60^\circ$$

Now, the turn load is calculated as

$$\phi = \cos^{-1}\left(\frac{1}{n}\right)$$

Rate of climb: As per CS 23.2120, for Level 1 and Level 2 high speed aircrafts and all Level 3 and 4 aircrafts must satisfy the minimum performance which is a climb gradient at take-off of 4% and the climb speed not less than  $1.3 V_s$ . So, the average climb speed of the aircraft is  $v_{cl} = 76.38$  m/s.

Aspect ratio: The designers define aspect ratio at the prior stage of the design and it remains constant all along the design process. The similar design of BWB is studied [11,12] and the aspect ratio of 4.5 is chosen for the design.

Maximum velocity: As suggested by Sadraey [13] can be calculated as

$$V_{max} = 1.25 V_c$$

Thus, the maximum velocity of the aircraft is 104.1 m/s. Similarly, CS 23. 335 suggest that cruising velocity of the aircraft cannot exceed  $0.9 V_{max}$  i.e 94 m/s. Since, the cruising speed of the aircraft is 83.3 m/s, it is in compliance with the established guidelines.

Lift and drag coefficient: The preliminary estimation of aerodynamic coefficients like  $C_{Dmin}$ ,  $C_{D,TO}$ ,  $C_{L,TO}$  etc. is done by studying the data on similar airfoil configurations available in the literature [14,15,16,17,18].

$$C_{Dmin} = 0.015$$

$$C_{D,TO} = 0.04$$

$$C_{L,TO} = 1.6$$

$$C_{L,max} = 1.1$$

#### D. Constraint analysis

It focuses on finding the optimal design point by evaluating the relationship between disc loading, power loading and wing loading which enables researchers to access the wing area requirements, rotor size and power requirements. In the methodology mentioned by author [14], the aircraft performance characteristics during the flight are

transformed in relation where power loading is the function of wing loading with the help of simplified drag model.

$$\left(\frac{W}{P}\right) = f\left(\frac{W}{S}\right)$$

The modified mathematical formulation of these equations for various phases of flight are referenced from [1] and [14].

The power loading for maintaining the particular bank load factor ( $n$ ) at a particular airspeed and altitude is obtained as

$$\frac{W}{P} = \frac{1}{\left[q \cdot \left\{ \frac{C_{Dmin}}{\left(\frac{W}{S}\right)} + k \left(\frac{n}{q}\right)^2 \cdot \left(\frac{W}{S}\right) \right\}\right]} \cdot \frac{v_{turn}}{550 \cdot \eta_{0,turn}}$$

where,  $C_{Dmin}$  is coefficient of minimum drag,  $k$  is lift-induced drag constant and  $\eta_{0,turn}$  is the overall efficiency of the propulsion system during turn.

The power loading required for climbing at a certain rate at certain altitude is obtained as

$$\frac{W}{P} = \frac{1}{\left[\frac{v_{cl}}{v} + \frac{q}{W} \cdot C_{Dmin} + \frac{k}{q} \cdot \frac{W}{S}\right]} \cdot \frac{v}{550 \cdot \eta_{0,cl}}$$

Similarly, the power required for decent can be calculated as below

$$\left(\frac{W}{P}\right)_{des} = \left(\frac{W}{0.2P}\right)_{cr}$$

In case of eVTOL aircraft, hover performance of ducted fan eVTOL aircraft can be analyzed with the help of disc actuator theory modified for ducted fan [1].

$$\left(\frac{W}{P}\right) = 2 \cdot \eta_{0,h} \cdot 550 \cdot \sqrt{\frac{\rho h}{A}}$$

where  $\eta_{0,h} = \eta_{B,h} \cdot \eta_{PE,h} \cdot \eta_{M,h} \cdot \eta_{F,h} \cdot \eta_{D,h}$  is the overall aircraft efficiency during hover,  $A_{j,h}$  is the total jet area during hover. Here, rotor disc area  $A$  is  $A = N \cdot A_{j,h}$ .

Similarly, the power requirement for achieving designed cruising speed at a particular altitude is obtained as

$$\frac{W}{P} = \frac{1}{\left[q \cdot C_{Dmin} \cdot \left(\frac{1}{W/S}\right) + k \cdot \left(\frac{1}{q}\right) \cdot \left(\frac{W}{S}\right)\right]} \cdot \frac{v_{cr}}{550 \cdot \eta_{0,cr}}$$

The power requirement for establishing the given service ceiling condition with the assumption of rate of climb of aircraft equivalent to 100 fpm is given as

$$\frac{W}{P} = \frac{1}{\left[ \frac{v_{cl}}{\sqrt{\frac{2}{\rho} \cdot \frac{W}{S} \cdot \sqrt{\frac{k}{3 \cdot C_{Dmin}}}}} + 4 \cdot \sqrt{\frac{k \cdot C_{Dmin}}{3}} \right]} \cdot \frac{v_{cl}}{550 \cdot \eta_{0,cr}}$$

where,  $\rho$  is air density at desired altitude

The power requirement for transitional flight is calculated by modifying the equation for power during hover phase as

$$\left(\frac{W}{P}\right)_{tr,avg} = \left[\left(\frac{W}{P}\right)_h + \left(\frac{W}{P}\right)_{tr,eff}\right] / 2$$

In case of hover power requirement, above equation becomes

$$\left(\frac{W}{P}\right)_{tr,avg} = \left(\frac{W}{0.55 \cdot P}\right)_h$$

This mathematical formulation is implemented in the form of python code to get constraint analysis plot which is the basis of the selection of optimal design point.

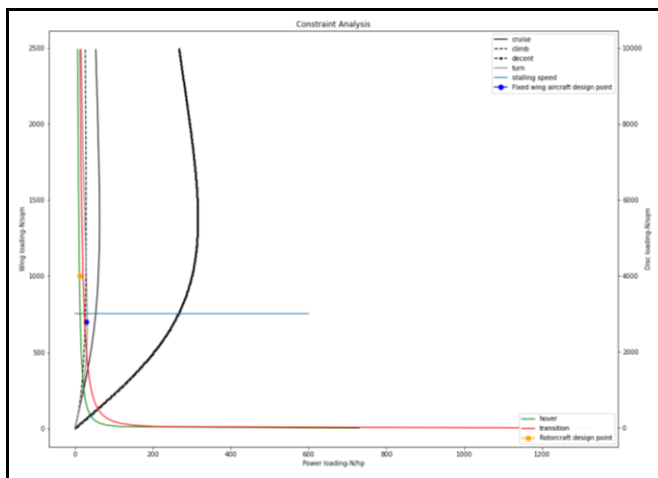


Fig. 3 Constraint analysis plot

The wing loading of  $700 \text{ N/m}^2$ , disc loading of  $4000 \text{ N/m}^2$  and power loading of  $12 \text{ N/hp}$  is selected for the design from constraint analysis. The power loading is selected based on the hover power requirement to ensure its capability for vertical take-off and landing. The disc loading for the design will be further optimized when assessment on feasibility of ducted fans and noise assessment is done in later stage of the research. The selected wing loading is enough to achieve the stalling speed recommended by CS 23 regulations relating to maximum coefficient of lift. The selected values of disc loading, wing loading and power loading will be the basis of sizing of ducted fans, wing and propulsion systems.

#### E. Aircraft initial geometry design and wing sizing

The preliminary requirements for wing design are influenced by various performance parameters, flying responses as well as structural responses.

**Wing Size:** The size of outer wing of BWB aircraft is influenced by overall geometry of the fuselage and the thickness is influenced by the requirement of cabin volume in order to accommodate for payload. The reference area of the BWB aircraft [19,20] can be defined as

$$S_{ref} = S_f + 2S_w$$

where,  $S_f$  is the reference area of the fuselage and  $S_w$  is the outer wing planform area. Determination of reference wing area is based on wing loading value determined through constraint analysis which gives its value as  $45.77 \text{ m}^2$ .

$$\frac{W}{S_{ref}} = 700 \text{ N/m}^2$$

Similarly, the gross aspect ratio for BWB aircraft is chosen based on literature and maximum wing span that can be imposed at certification and is defined as

$$AR = \frac{b^2}{S_{ref}} = 4.5$$

where,  $b$  is the total reference wing span from one wing tip to the other. This enables designers to calculate the total reference wing span of the design which is  $14.25 \text{ m}$ .

**Wing Sweep:** The primary goal of the wing sweep is to improve aerodynamic features like lift, drag, pitching moment and increase critical Mach number. It also provides us with option of incorporating vertical tails at wingtips by increasing tail effectiveness thus improving directional and longitudinal stability. By sweeping the wing backward and including washout, the wingtips lie behind the aerodynamic center and at zero lift, produce a downward force while the inner portion of the wing is lifting, thus producing a positive  $C_m$  at zero lift and hence about the aerodynamic center at all coefficient of lift [21].

**Taper Ratio:** It is the ratio of the tip chord of wing to the root chord of the aircraft wing.

$$\lambda_w = \frac{C_t}{C_r}$$

Even though rectangular wing planform has some advantages in terms of performance, ease of manufacturing and cost, but it is aerodynamically inefficient. But with taper wing planform, designers can reduce the induced drag. The preliminary estimation of taper ratio  $\lambda_w$  the wing obtained from sweep angle and taper ratio relation and the value is selected so as to have near elliptical lift distribution.

**Preliminary Lift Distribution Calculation:** For preliminary assessment of lift distribution, Weissinger model [22] is used as our design is incorporating sweep greater than  $15^\circ$ . The mathematical model for this model implemented in python. It takes geometric angle of attack at root of the wing, wing span, root chord, tip chord, sweep and washout as input.



Similarly, outputs from the program are aspect ratio, wing planform area, mean aerodynamic chord, coefficient of lift and coefficient of induced drag. The variation of  $C_L$  and  $C_{Di}$  with the variation in  $\lambda$  and  $A$  calculated from Weissinger model is shown in Fig. 4 and Fig. 5 respectively.

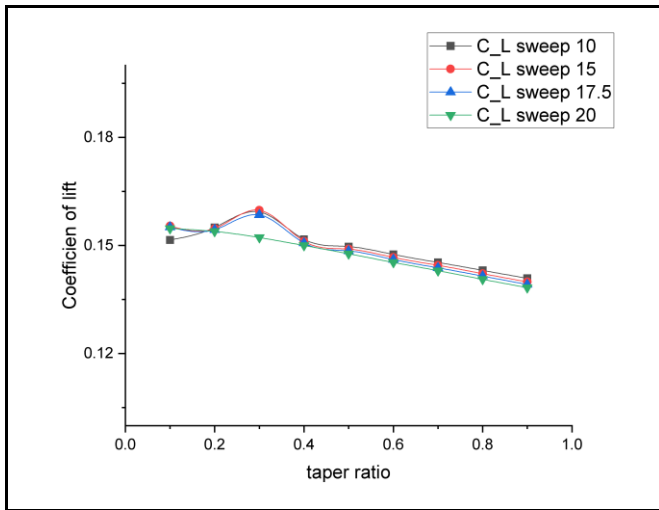


Fig. 4 Variation of Coefficient of Lift with taper ratio for different outboard sweep

It is clear that both taper ratio and wing sweep influence the distribution of lift across the wing. The increase in taper ratio resulted in the decrease in coefficient of lift. In terms of higher lift coefficient, optimum taper ratio is found to be between 0.2 and 0.4 for the chosen wing planform and aspect ratio but the higher value of taper ratio gave near elliptical lift distribution and low induced drag coefficient. Also, when the taper ratio of the wing is increased, it resulted in the decrease of induced drag for chosen wing planform. Moreover, increasing the wing sweep resulted in increasing coefficient of lift from  $10^\circ - 15^\circ$  but decreasing lift coefficient from  $15^\circ - 20^\circ$ .

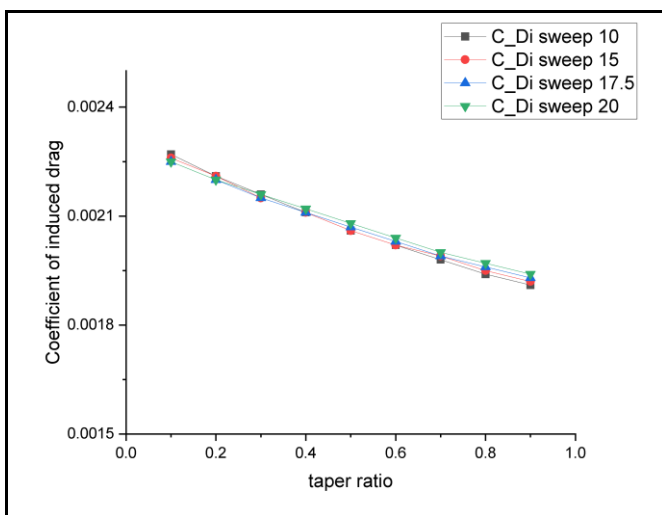


Fig. 5 Variation of Coefficient of induced drag with taper ratio for different outboard sweep

Based on these observations, for the outboard wing, the quarter chord sweep of  $25^\circ$  and taper ratio of 0.4 was selected for the wing of eVTOL BWB aircraft as it provide reasonably good lift to induced drag factor and acceptable lift and load distribution.

Similarly, the inboard wing is designed to carry payload as well as to generate lift. Most of the dimensions are chosen based on the volume requirement inside the cabin to adjust payload. Wing thickness ratio is decided by airfoil used for center body. For the early design of inboard wing (fuselage) taper ratio is chosen such that the root chord of the outer wing becomes equal to the tip chord of the inner wing. All the parameters associated with inboard and outboard wing design and presented in Table 2.

Table 2. Design parameters for outboard and inboard wings

Wing	$\Lambda_{c/4}$	$\Lambda_{LE}$	$\lambda$	$C_r$	$C_t$	AR	$S_{eff}$	$\theta$	$\alpha_{root}$
Inboard	$45^\circ$	$59^\circ$	0.5	8	4	0.5	18	0	0
Outboard	$25^\circ$	$29.8^\circ$	0.4	4	1.6	4	31.5	$2^\circ$	$3^\circ$

The cruising Mach number of aircraft is 0.253 and cruising Reynolds number of at different sections are given below which will be the basis of airfoil selection for our design.

$$Re_{inboard,r} = \frac{\rho \cdot v_{cr} \cdot C_{inboard,r}}{\mu_{cr}} = 35.42 \cdot 10^6$$

$$Re_{inboard,t} = \frac{\rho \cdot v_{cr} \cdot C_{inboard,t}}{\mu_{cr}} = 17.71 \cdot 10^6$$

$$Re_{outboard,r} = \frac{\rho \cdot v_{cr} \cdot C_{outboard,r}}{\mu_{cr}} = 17.71 \cdot 10^6$$

$$Re_{outboard,t} = \frac{\rho \cdot v_{cr} \cdot C_{outboard,t}}{\mu_{cr}} = 7.085 \cdot 10^6$$

The sweep angle chosen is smaller compared to typical BWB design data found in literature as they are associated with high subsonic or supersonic regime of operation. The lift and load distribution across the chosen outboard wing planform is presented in Fig. 6.

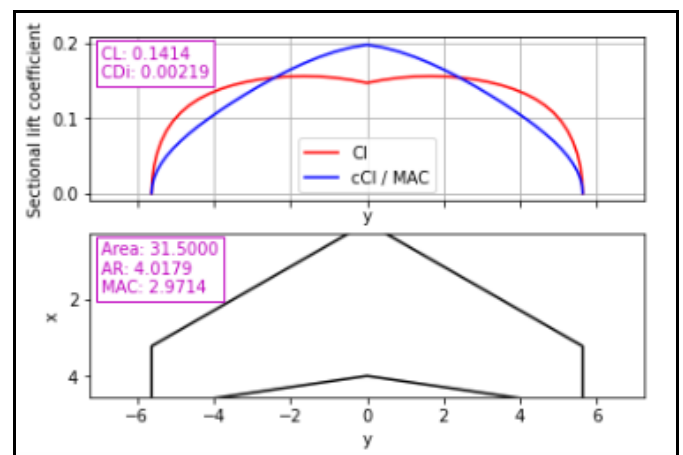


Fig. 6 Lift and load distribution over the outboard wing

### V. AIRFOIL ANALYSIS AND SELECTION

The choice of airfoils for aircraft begins with a precise definition of the required flight performance. The criteria for the selection of inboard section airfoils are different from that of outboard wing. The airfoil section for inboard section is influenced by cabin volume requirement for the aircraft. Similarly, the stability and control become other important aspect of airfoil section for the eVTOL BWB tailless aircraft.

#### A. General Requirements

In general, following characteristics are considered during the airfoil selection.

- Coefficient of Moment  $C_m \approx 0$  or positive
- Coefficient of Lift  $C_l$  as high as possible
- Thickness to chord ratio  $t/c$  large enough to provide cabin volume requirements
- Elliptical spanwise lift distribution by proper selection of airfoil spanwise twist.

Considering the BWB requirement, it is decided to use reflex airfoil for center portion and cambered airfoil for outboard wing with proper distribution of sweep and twist. This ensures satisfaction of stability requirements from the combination of reflex airfoil and wing twist and high lift requirement from outboard wing cambered airfoils. It is important to keep in mind that optimal choice of airfoil for the studied configuration is the one with lower pitching moment coefficient as it decreases the extent of twist requirement providing greater flexibility for speed without compensating too much on off design point [23]. The eVTOL BWB aircraft cruise lift coefficient and maximum lift coefficient are given as

$$C_{Lcr} = \frac{2 \cdot MTOW}{Q_{cr} \cdot v_{cr}^2 \cdot S_{eff}}$$

$$C_{Lmax} = \frac{2 \cdot MTOW}{Q_s \cdot v_s^2 \cdot S_{eff}}$$

$$S_{eff} = S_{inboard\ wing} + S_{outboard\ wing} = 49.5\ m^2.$$

Thus, the required cruise lift coefficient for our BWB eVTOL aircraft is  $C_{Lcr} = 0.207$  and the required maximum lift coefficient of the wing body combination is  $C_{Lmax} = 0.942$ .

#### B. Inner Body Airfoil Selection

The airfoils for BWB aircraft center body design selected for comparison are MH 78, HS 533, NACA 23112, LA2573 A and Eppler 635 with 18% thickness. The batch analysis is done in XFLR software for angle of attack in the range of  $-20^\circ$  to  $20^\circ$  and Reynolds number in the range of  $7.10^6$  to  $1.8 \cdot 10^7$  at operating Mach number of 0.25. Fig. 7 to 11 show the variation of aerodynamic parameters for different airfoils.

In Fig. 7, it is observed that HS 522 airfoil has maximum value of zero lift coefficient as well as higher value of lift

coefficient for given angle of attack. But NACA 23112 and MH 78 have efficient operation characteristics for higher angle of attack owing to their higher stalling angle. Similarly, the highest value of coefficient of lift is obtained from MH78 at  $19^\circ$ . With the increase in Reynolds number, the aerodynamic properties stay same with slight variation.

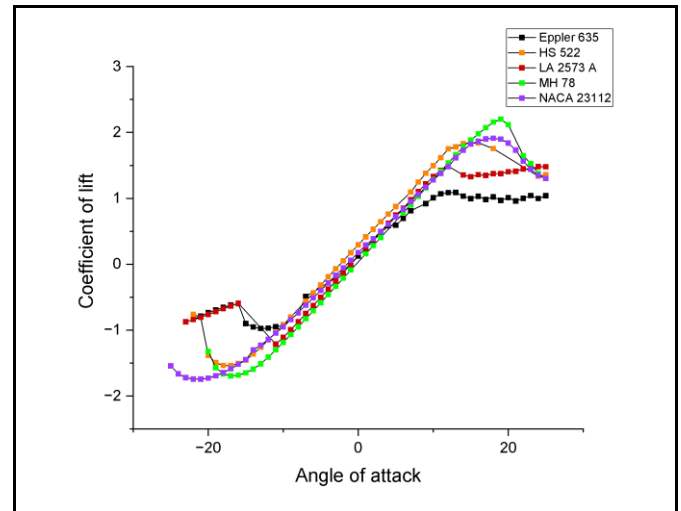


Fig. 7 Variation of Coefficient of Lift with angle of attack for inboard airfoils at Reynolds number 1.6 million and  $M=0.25$

Similarly, LA 2573A and MH 78 have maximum values of Lift to Drag ratio which is shown in Fig 8. But the lift to drag ratio for LA 2573A is reducing drastically at higher angle of attack with the onset of stall. NACA 23122 proves to be safer for operating at higher angle of attack since the lift to drag ratio is reducing gradually rather than unstable stall behavior. Most of the chosen airfoils exhibit low drag properties between the angle of attack range  $-10^\circ$  to  $10^\circ$  as shown in Fig 9. NACA 23112 is excellent airfoil choice in terms of low drag as it shows low drag characteristics even up to  $15^\circ$ .

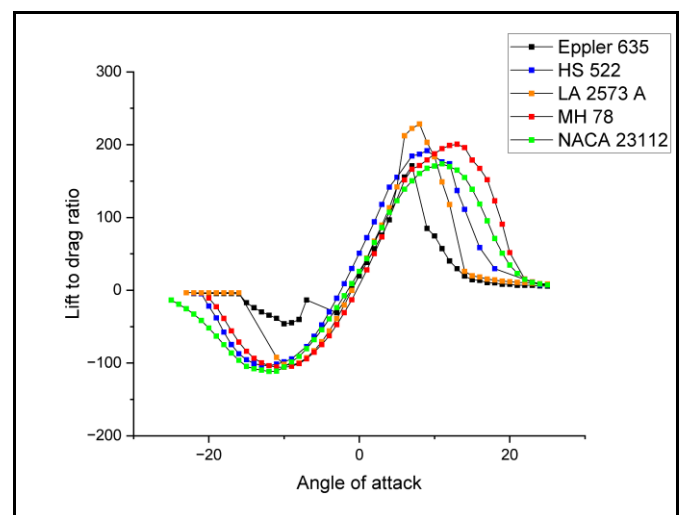


Fig. 8 Variation of Lift to Drag ratio with angle of attack for inboard airfoils at Reynolds number 1.6 million and  $M=0.2$

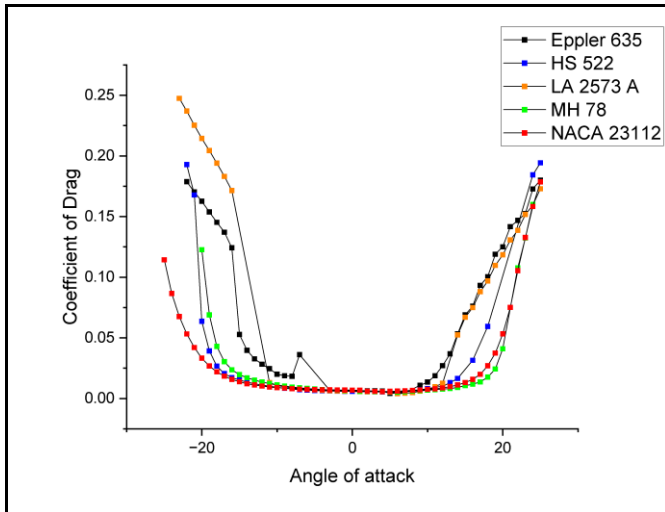


Fig. 9 Variation of Coefficient of Drag with angle of attack for inboard airfoils at Reynolds number 1.6 million and  $M=0.25$

Fig. 10 shows the variation of lift coefficient with drag coefficient for different angle of attack. This graph has unique bucket characteristics associated with its shape. MH78 and NACA 23112 show excellent characteristics from drag bucket as they provide pilot for the option of operating at lowest drag point while varying coefficient of lift.

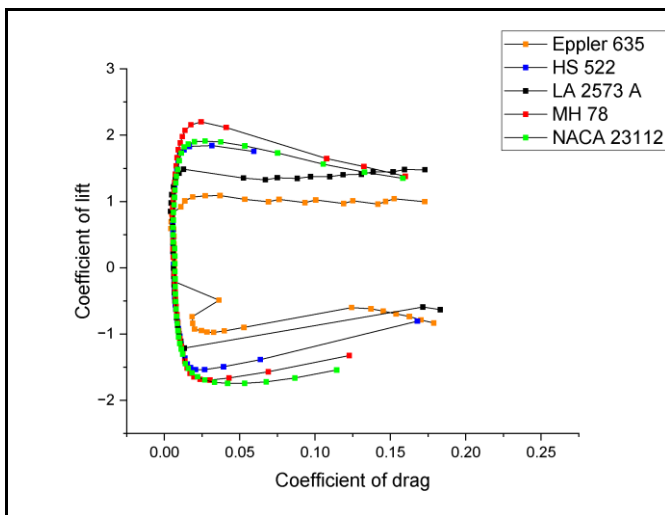


Fig. 10 Variation of Coefficient of Drag with Lift for inboard airfoils at Reynolds number 1.6 million and  $M=0.25$

Fig. 11 shows the variation of pitching moment coefficient of airfoil with angle of attack. The pitching moment for NACA 23112 is almost equal to zero for the range of angle of attack from  $-5^\circ$  to  $5^\circ$ . The design objective is to have  $C_m$  close to zero. So, NACA 23112 is best for control and stability of the intended design. Also, MH 78 has desirable aerodynamic properties along with NACA 23112. Because of pitching moment characteristics, NACA 23221 is chosen for tip section of center body while MH 78 is chosen for root section of the center body for eVTOL BWB aircraft design.

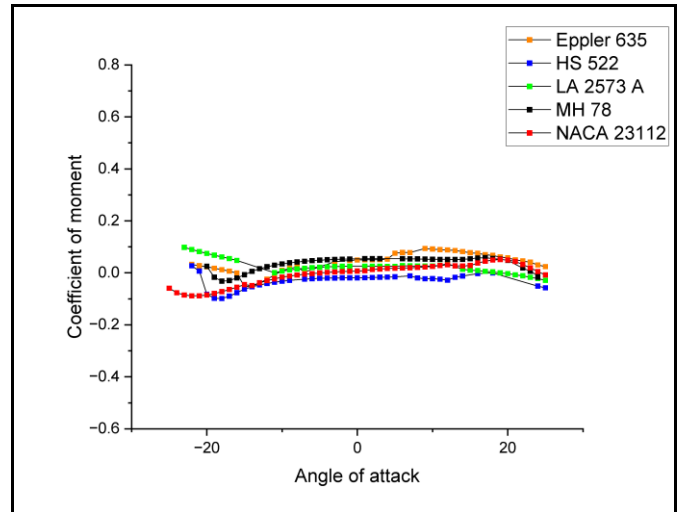


Fig. 11 Variation of pitching moment with angle of attack for inboard airfoils at Reynolds number 1.6 million and  $M=0.25$

### C. Outer Wing Airfoil Selection

The outer board wing of the airfoil is crucial part of the design since majority of the lift of the aircraft is generated by this section. Moreover, it should have capability to counteract the negative pitching moment created due to center body airfoils thereby resulting in positive pitching moment for overall stability and control of the aircraft. The airfoils for BWB aircraft outer wing design selected for comparison are Worthmann FX 60-126, GOE 440, MH 115, FX 61-140 and Eppler 395. Their aerodynamic characteristics are studied with Reynolds number in the range of  $7.10^6$  to  $1.8 \cdot 10^7$ .

FX 60-126 and MH 115 have similar values for maximum lift coefficient as seen from Fig. 12. But the stalling behavior of MH 115 is better than that of FX 60-126. Similarly, Eppler 395 and MH 115 have highest value for lift to drag ratio. Also, FS 60-126 has comparatively low lift to drag ratio but it is constant rather than decreasing in the range of  $4^\circ$  to  $10^\circ$  AOA.

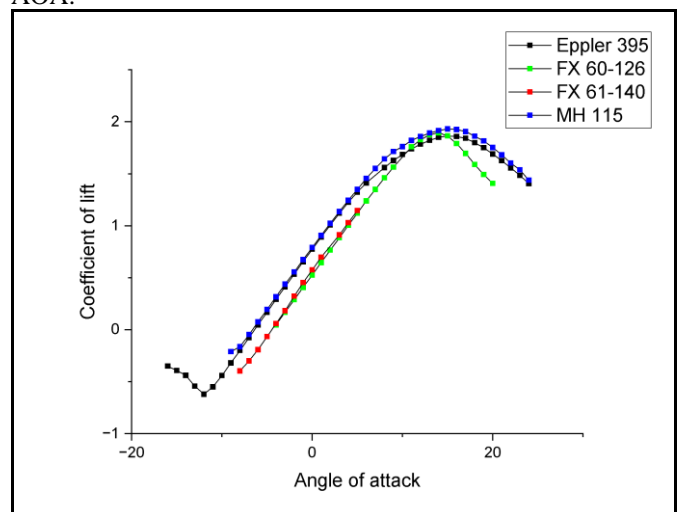


Fig. 12 Variation of Coefficient of Lift with angle of attack for outboard airfoils at Reynolds number 0.7 million and  $M=0.25$

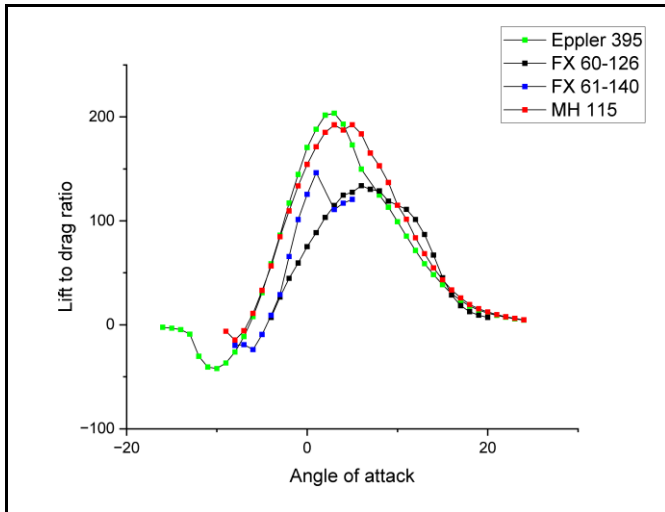


Fig. 13 Variation of Lift to Drag ratio with angle of attack for outboard airfoils at Reynolds number 0.7 million and M=0.25

The drag coefficient is almost constant for the angle of attack of range  $-10^{\circ}$  to  $10^{\circ}$ , which resembles the observation made for airfoils selected for inner body design. It is shown in Fig 14. Also, the drag bucket characteristics for all the selected airfoils are promising with Eppler 395 offering constant minimum drag coefficient at angle of attack increases, which is shown in Fig. 15.

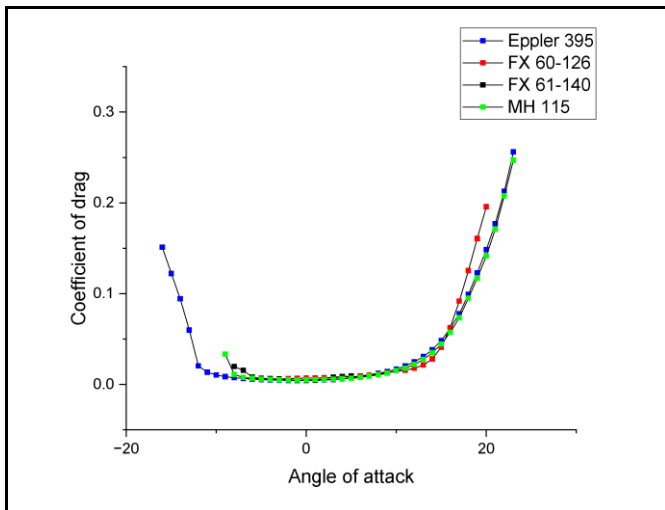


Fig. 14 Variation of Coefficient of Drag with angle of attack for outboard airfoils at Reynolds number 0.7 million and M=0.25

Similarly, Fig. 16 shows the variation of pitching moment coefficient of airfoils selected for outboard wings with angle of attack. MH 115 and Eppler 395 have highly negative pitching moment coefficient of around 0.18 at  $0^{\circ}$  angle of attack. Similarly, FX 60-126 has the negative pitching moment coefficient of 0.12 at  $0^{\circ}$  angle of attack. Overall aerodynamic performance of MH 115 is good except for slightly greater value of pitching moment coefficient compared to FX 60-126. So, MH 115 is selected for tip of outer wing and final assessment will be made after high fidelity CFD studies. Thus, the airfoils selected for the design

of eVTOL BWB aircraft are: MH 78 (modified for 18% thickness) for root section of center body, NACA 23112 for tip section of center body and MH 115 for tip section of outer wing.

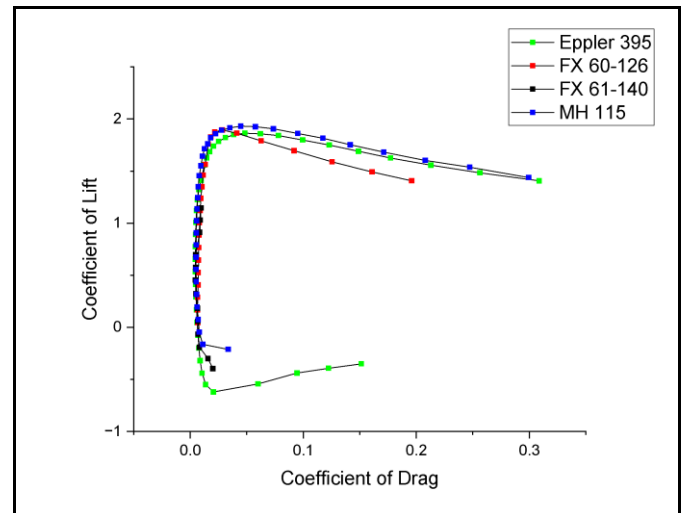


Fig. 15 Variation of Coefficient of Lift with Coefficient of Drag for outboard airfoils at Reynolds number 0.7 million and M=0.25

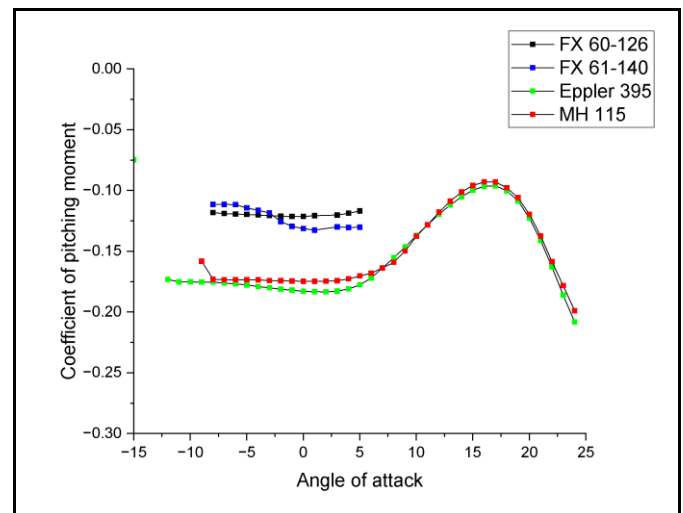


Fig. 15 Variation of pitching moment with angle of attack for outboard airfoils at Reynolds number 0.7 million and M=0.25

## VI. AIRCRAFT DESIGN AND PERFORMANCE ANALYSIS

### A. Aircraft Modelling

The airfoils selected in the above section are used for the design of BWB eVTOL initial 3-D model using wing and plane design module. The design details of the aircraft are presented in Table 3. Similarly, the designed aircraft model is presented in Fig. 16. Initially no twist and dihedral distribution is incorporated in the wing and their optimum values are determined by solving stability and lift distribution aspects of the aircraft using robust numerical methods and experimental investigations.



**Table 3.** Design details of aircraft model

Y Ypanel	Chord	Offset	Dihedral	Twist	Foil	Xpanel
0	8	0	0	0	MH 78	13
19						
0.25	7.85	0.15	0	0	MH 78	13
3						
0.5	7.5	0.5	0	0	MH 78	13
2						
1.5	4	4	0	0	NACA 23112	13
1.6	3.9	4.1	0	0	NACA 23112	13
2						
7.12	1.2	7.22	0	0	MH 115	

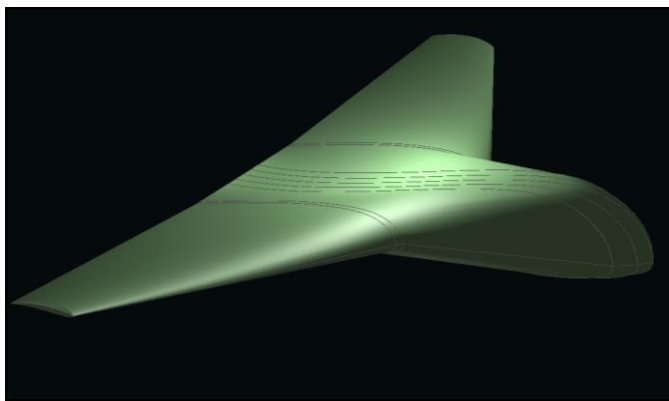


Fig. 16 eVTOL BWB aircraft model right side view

**B. Aerodynamic Performance Assessment**

The aerodynamic analysis of the aircraft was based on Ring vortex (VLM2) viscous analysis. The free stream velocity of 83.3 m/s and Reynolds number range of  $7.10^6$  to  $3.50^7$  was used for performance assessment.

Fig. 17 to 20 show the variation of pressure coefficient with the change in angle of attack at  $-5^\circ$ ,  $0^\circ$ ,  $3^\circ$  and  $15^\circ$  respectively. At negative angle of attack of  $-5^\circ$ , there is higher positive value of coefficient on the aircraft due to large amount of airflow across the BWB aircraft but the coefficient of lift is negative.

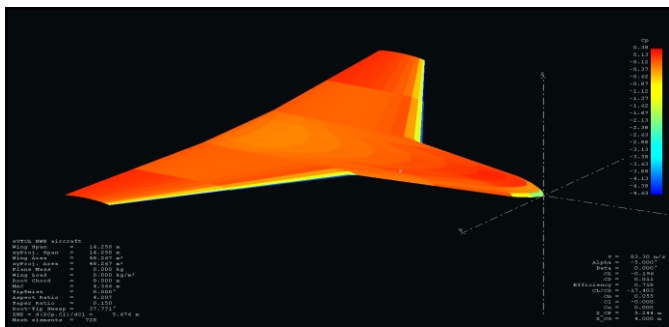


Fig. 17 Coefficient of pressure distribution on eVTOL BWB aircraft at  $-5^\circ$  angle of attack.

With increase in angle of attack to zero degrees, higher pressure coefficient is occurring at maximum thickness portion of the center body creating drag at lower angle of

attack. As the angle of attack is increased to  $3^\circ$ , height of suction peak increases leading to greater value of pressure coefficient at leading edge section of outer wing whereas, moderate pressure coefficient at leading edge of the center body. This reduces overall drag as well. This configuration provides good lift to drag ratio and lift coefficient obtained at this angle of attack is sufficient for cruising flight of the aircraft. When the angle of attack is increased to  $15^\circ$ , flow separation occurs at the trailing edge of the wing and moves upward thereby destroying suction peak. This results in increase in drag and decrease in coefficient of pressure.

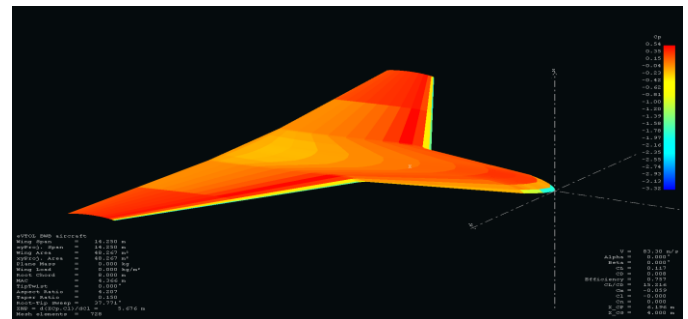


Fig. 18 Coefficient of pressure distribution on eVTOL BWB aircraft at  $0^\circ$  angle of attack.

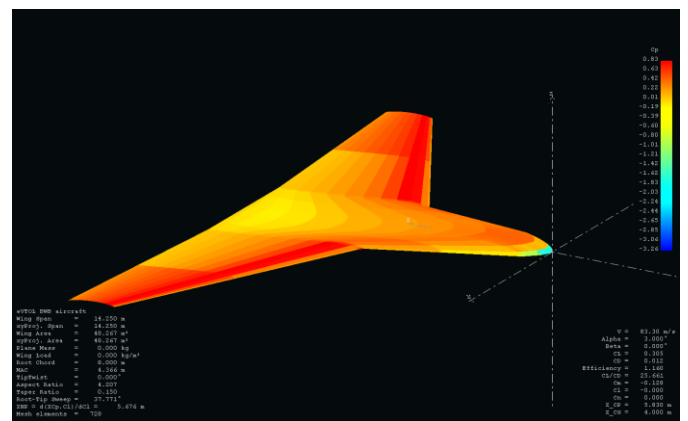


Fig. 19 Coefficient of pressure distribution on eVTOL BWB aircraft at  $3^\circ$  angle of attack.

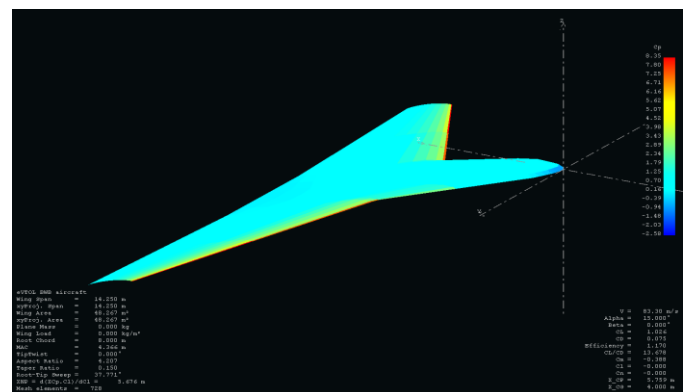


Fig. 20 Coefficient of pressure distribution on eVTOL BWB aircraft at  $15^\circ$  angle of attack.

The variation of local lift distribution with angle of attack for the eVTOL BWB aircraft is presented in Fig. 21. Higher

amount of lift is obtained at all spanwise location with the increase in angle of attack. At lower angle of attack, the lift generated at all spanwise location is almost similar including the center body location. This reduces the lift dependency only on outer wings unlike conventional design. But at higher angle of attack, the lift generated by outer wing is decreased as we move along spanwise location from root to tip of the aircraft.

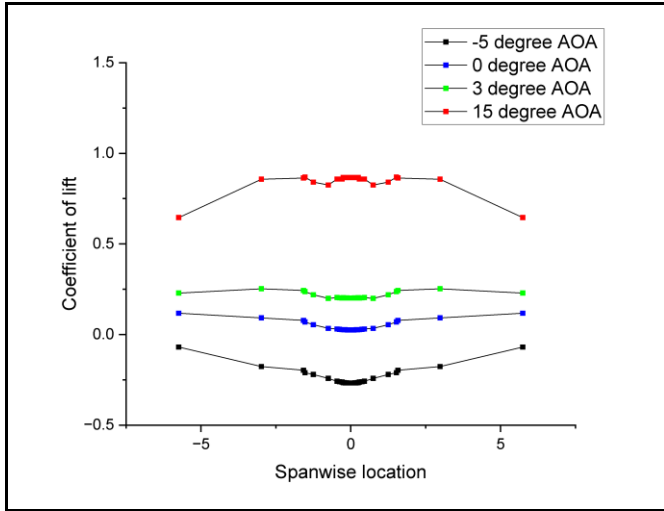


Fig. 21 Variation of local lift distribution for eVTOL BWB aircraft with angle of attack

The variation of induced drag along spanwise location with change in angle of attack is presented in Fig. 22. Increase in angle of attack results in increased induced drag for at every spanwise location. The increase is maximum at outer wing tips and it decreases as we move to the center body location. This poses a constraint on design on choosing effective angle of attack for cruise which provide optimal performance rather than focusing only on higher value of lift coefficient.

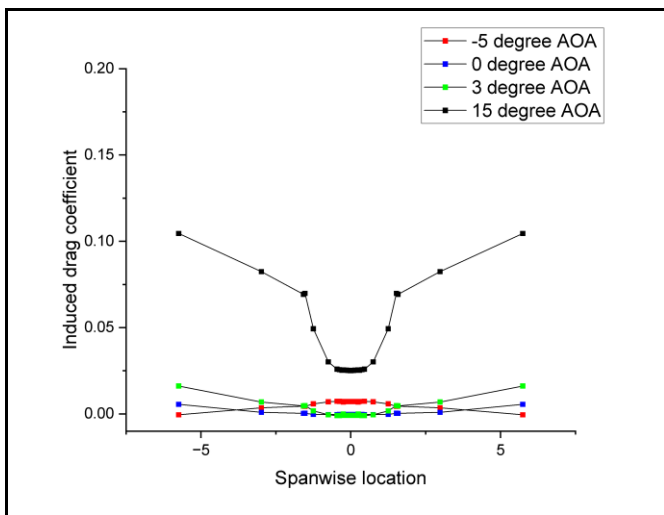


Fig. 22 Variation of induced drag coefficient for eVTOL BWB aircraft with angle of attack

The polar analysis on cruising phase of flight is performed to access the performance characteristics of the design in detail. Fig. 23 shows the variation of lift to drag ratio with angle of attack at cruising Mach number of 0.253. The maximum value of lift to drag is 25.66 which is obtained at cruising angle of attack of 3°. As per the constraint analysis  $C_{Lcr} = 0.207$  was required and the lift coefficient of aircraft at 3° is obtained to be 0.304 from polar analysis. Thus, the design meets the design requirement for cruising phase of the flight.

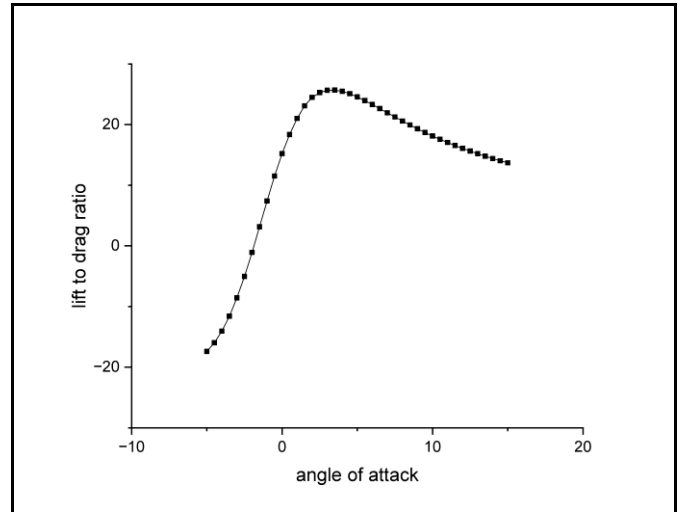


Fig. 23 Variation of lift to drag ratio for eVTOL BWB aircraft with angle of attack at cruising phase of the flight

The higher coefficient for lift for certain conditions can be obtained by increasing angle of attack beyond 3°. It is shown in Fig 24. But it comes at the cost of extra drag. This exponential increase in drag coefficient with increase in angle of attack is shown in Fig. 25. The maximum coefficient of lift required for satisfying the stalling speed requirement was calculated to be 0.942 which can be attainable at 13.5° AOA.

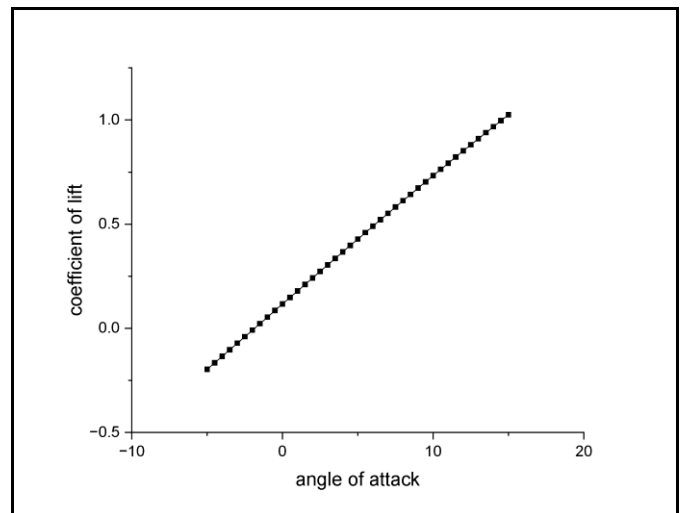


Fig. 24 Variation of coefficient of lift for eVTOL BWB aircraft with angle of attack at cruising phase of the flight

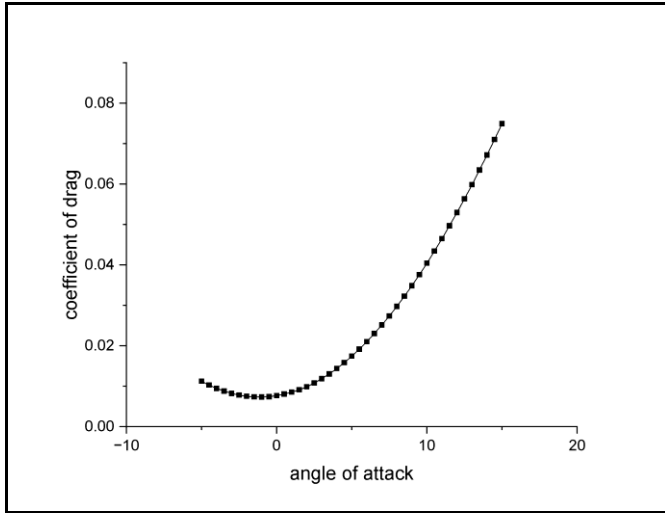


Fig. 25 Variation of coefficient of drag for eVTOL BWB aircraft with angle of attack at cruising phase of the flight

The coefficient of drag for cruising phase of the flight is equal to 0.011885 which is obtained from Fig. 25. With reference to data from BWB aircraft literature, the minimum drag coefficient of  $C_{Dmin} = 0.015$  was taken for the design. From aerodynamic assessment as shown in Fig. 27, it is found to be  $C_{Dmin} = 0.007363$ , which suggest a great improvement in design.

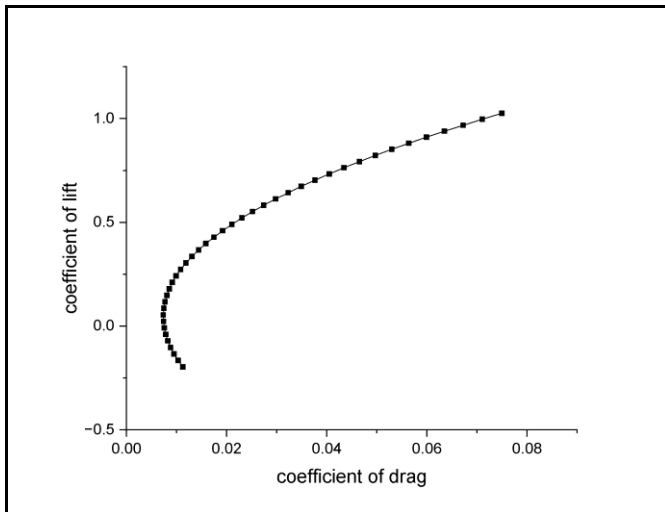


Fig. 26 Variation of coefficient of drag with coefficient of lift for eVTOL BWB aircraft at cruising phase of the flight

The variation of pitching moment of the aircraft with angle of attack is shown in Fig. 27. At the cruising angle of  $3^\circ$ , the pitching moment coefficient of aircraft is  $-0.127$ . Negative pitching moment coefficient is desirable for cruising condition as it helps counterbalance nose up moment resulted due to disturbance in flight such as turbulence and is favorable for aircrafts with high lift coefficient. Thus, the preliminary design of aircraft owing to its fundamental calculations of forces and moments is completed in this section.

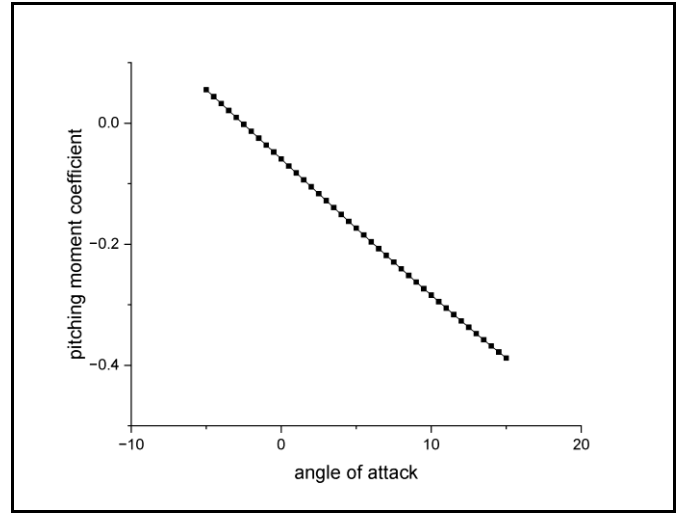


Fig. 27 Variation of pitching moment coefficient for eVTOL BWB aircraft with angle of attack at cruising phase

## VII. PROPULSION, POWER AND ENERGY REQUIREMENTS

### A. Battery capacity

Wing loading of  $700 \text{ N/m}^2$ , disc loading of  $4000 \text{ N/m}^2$  and power loading of  $12 \text{ N/hp}$  was selected for the design of eVTOL BWB aircraft in reference to constraint analysis. The design and sizing of wing, ducted fans and propulsion system is to be carried on the basis of these values of wing loading, disc loading and power loading. In taking in to consideration the technological advancement level of battery capacity during the period of development, the initial estimation of battery energy density of  $E^* = 400 \text{ Wh/Kg}$  is made. With the ratio of battery mass to MTOM of  $\mu_b = 0.3$ , the total stored energy for the propulsion requirement is calculated as

$$E_s = \mu_b \cdot MTOM \cdot E^* = 391.92 \text{ kWh}$$

### B. Energy Requirement for Each Phase

The power requirement for hover and transition flight are calculated from Rotorcraft design point i.e from the selected disc loading. Similarly, the power requirements for cruise, turning and decent flight are calculated from the fixed wing aircraft design point i.e from the selected wing loading obtained from constraint analysis. The result of the power requirement is presented in Table 4.

Table 4. Power requirement for each flight phase

Phases	Power loading (N/kW)	Total power (kW)
Hover	15.48	2068.55
Climb	35.05	914.04
Cruise	68.35	468.73
Decent	341.76	93.74
Transition	28.16	1137.71

The power requirements for hover and transition flight are greater than other phases of flight but the cruise power requirement is minimal for ducted fan configuration. Since,

majority of the flight mission is cruise phase and only a small amount of time is spent for hovering and transition flight, so overall power requirement is minimized for the design.

### C. Range Assessment

The range assessment of the aircraft is made based on mission profiles and expected time duration of each of the mission segment. This assessment gives designer the idea of whether or not the range requirement of the intended eVTOL aircraft can be achieved with the power requirements and total energy stored in the battery. The range of the aircraft is calculated on the basis of power requirement calculated for each phase of the flight. The overall range of the aircraft is calculated as

$$R = \frac{v_{cr}}{P_{cr}} \cdot (E_s(1 - SOC_{min}) - t_h \cdot P_h - 2 \cdot t_{tr} \cdot P_{tr} - t_{cl} \cdot (P_{cl} + P_{des})) + 2 \cdot t_{cl} v_{cl}$$

where,  $E_s$  is the total stored energy in the battery,  $SOC_{min}$  is the minimum allowable state-of-charge which is taken at 10%.

The derivation of the above equation is given in [1]. The time duration of each phase for a typical flight mission is presented in Table 5.

Table 5. Time duration for each flight phase

Phases of flight (seconds)	Time
Take-off hover phase	15
Transition phase	20
Climb phase	200
Cruise phase	$t_{cr}$
Descent phase	200
Re-transition phase	20
Landing hover phase	45

## VIII. CONCLUSIONS AND FUTURE WORK

In this paper, the preliminary design of BWB eVTOL aircraft suited for UAM and RAM market has been successfully carried out. Existing mathematical models are modified for their applicability to the suggested unconventional design. Similarly, the initial framework is developed to carry the systematic preliminary design and performance assessment which is capable of offering designer appropriate guidance for designing blended wing body configuration without having to dive into complicated numerical investigation approach at initial stage of the design. Similarly, the benefit of incorporating BWB configuration for vertical take off and landing electric aircraft is clearly identified in terms of its aerodynamic benefits. But in-depth assessment on stability as well as control response of the aircraft is required to understand if this configuration is optimal for next generation of electric VTOL aircrafts. Some of the future works based on this research would include understanding the complexity of ducted fans on the integration of BWB configuration, detail understanding on structural integrity, aerodynamic interactions and propulsion

system as well as the development of the architecture for distributed electric propulsion.

## REFERENCES

- [1] Nathen, P., Bardenhagen, A., and Taylor, J. "Architectural Performance Assessment of an Electric Vertical Take-off and Landing (e-VTOL) Aircraft Based on a Ducted Vectored Thrust Concept."
- [2] Liebeck, R. H. "Design of the Blended Wing Body Subsonic Transport." *Journal of Aircraft*, Vol. 41, No. 1.
- [3] Olcott, D. D. "Tri-Fan VTOL Conceptual Design." 2016. <https://doi.org/10.2524/6.2016-3610>.
- [4] Finder, D. F., Braun, C., and Nil, C. "Impact of Electric Propulsion Technology and Mission Requirements on the Performance of VTOL UAVs." *CEAS Aeronautical Journal*, Vol. 10, 2019, pp. 827-843.
- [5] Duffy, M. J., Wakayama, S., Hupp, R., Lacy, R., and Stauffer, M. "A Study in Reducing the Cost of Vertical Flight with Electrical Propulsion." 17<sup>th</sup> AIAA Aviation Technology, Integration, and Operations Conference, 2017. <https://doi.org/10.2514/6.2017-3442>.
- [6] Polaczyk, N., Trombino, E., Wei, P., and Mitici, M. A. "A Review of Current Technology and Research in Urban On-Demand Air Mobility Applications." 8<sup>th</sup> Biennial Autonomous VTOL Technical Meeting and 6<sup>th</sup> Annual Electric VTOL Symposium 2019, 2019, pp. 333-343
- [7] Rob, McDonald, Patterson, M., Gohardani, A., Langelaan, J., and Hepperle, M. "Misconceptions of Electric Propulsion Aircraft and Their Emergent Aviation Markets." 2014.
- [8] Smith, J. C., Viken, J. K., Guerreiro, N. M., Dollyhigh, S. M., Fenbert, J. W., Hartman, C. L., Kwa, T. S., and Moore, M. D. "Projected Demand and Potential Impacts to the National Airspace System of Autonomous, Electric, on-Demand Small Aircraft." 12<sup>th</sup> AIAA Aviation Technology, Integration and Operations (ATIO) Conference and 14<sup>th</sup> AIAA/ISSMO Multidisciplinary Analysis and Optimization Conference, 2012. <https://doi.org/10.2514/6.2012-5595>.
- [9] Bacchini, A., and Cestino, E. "Key Aspects of Electric Vertical Take-off and Landing Conceptual Design." <https://doi.org/10.1177/0954410019884174>, Vol. 234, No. 3, 2019, pp. 774-787. <https://doi.org/10.1177/0954410019884174>.
- [10] Raymer, D. P. "Aircraft Design: A Conceptual Approach." 2012, p. 1044.
- [11] TU Berlin, D. of A. D. and A. "Efficiency Meets Sky, Joint NASA/SLR Aeronautics Design Challenge 2017-2018." 2018.
- [12] Humphreys-Jennings, C., Lappas, I., and Sovar, D. M. "Conceptual Design, Flying, and Handling Qualities Assessment of a Blended Wing Body (BWB) Aircraft by Using an Engineering Flight Simulator." *Aerospace* 2020, Vol. 7, Page 51, Vol. 7, No. 5, 2020, p. 51. <https://doi.org/10.3390/AEROSPACE7050051>.
- [13] Sadraey, M. H. "Aircraft Performance: An Engineering Approach."
- [14] Snorri, G. "General Aviation Aircraft Design: Applied Methods and Procedures", 2018.
- [15] Ahmet, A. "MANTA-NASA DLR Aeronautical Design Challenge", 2021.
- [16] Sam, D., Oliver, J. "Aerodynamic Design and Exploration of a Blended Wing Body Aircraft at Subsonic Speed", *International Journal of Aviation, Aeronautics, and Aerospace*, 6(5). <https://doi.org/10.15394/ijaaa.2019.1411>.
- [17] Nimeesha, B.K. "Aerodynamic Shape Optimization of a Blended-Wing-Body Aircraft Configuration", Master Thesis. 2011.
- [18] Sathvik, S.R. "Conceptual Design of a Blended Wing Body Aircraft for Urban Air Mobility Operation", Master's Thesis. 2019.
- [19] Struber, H. and Hepperle, M. "Aerodynamic Optimisation of a Flying Wing Transport Aircraft", Springer. doi:10.1007/978-3-540-33287-9 9.
- [20] Pitera, D. M., DeHaan, M., Brown, D., Kawai, R. T., Hollowell, S., Camacho, P., Bruns, D., and Rawden, B. K. "Blended Wing Body Concept Development with Open Rotor Engine Integration," Tech. Rep. NASA/CR2011-217303, Boeing and NASA. 2011.
- [21] Ilan, K. "Tailless Aircraft Design-Recent Experiences", Symposium on Aerodynamics & Aeroacoustics, Tucson, AZ, March 1-2, 1993.
- [22] Weissinger, J. "The lift distribution of swept-back wings", NASA Technical Memorandum NO. 1120, 1947.
- [23] Randhir, B. "Design of a Blended Wing Body Aircraft", San Hose State University, Masters thesis. 2014.